Indonesian Journal of Electrical Engineering and Computer Science
Vol. 41, No. 3, March 2026, pp. 859~872
ISSN: 2502-4752, DOI: 10.11591/ijeecs.v41.i3.pp859-872

Overvoltage assessment of wind energy integration in low voltage distributed grids

Farid Merahi[1], Badoud Abd Essalam[2]
[1]Department of Electrical Engineering, University Setif 1- Ferhat Abbas, Setif, Algeria
[2]Department of Automatic and Intelligent Systems, University Setif 1- Ferhat Abbas, Setif, Algeria

Article Info

Article history:

Received Oct 15, 2025
Revised Jan 21, 2026
Accepted Feb 27, 2026

Keywords:

LV distributed network
Overvoltage assessment
Wind energy in power system
Wind energy integration impact

ABSTRACT

Large-scale integration of renewable energy (RE) resources into the electrical grid has increased significantly over the last decade, affecting the network at various nodes even at considerable distances from the common connection point. This paper presents an overvoltage assessment caused by the integration of two wind generators (WGs) into a low voltage distribution grid, which is structured into three zones. Two scenarios are studied, the first one considers the low voltage grid without WGs, representing its natural operating condition. In the second scenario, two WGs are connected in zone 3, inducing voltage rises at different nodes within the same zone, by reaching 7.9%, and affecting nodes located in other zones (Zone 1 and Zone 2). The simulation is performed using MATLAB/Simulink (R2025a), and the results obtained are compared to the standards test feeder IEEE 33-bus network, showing the overvoltage caused by WGs integration at nodes close to the connection point while improving voltage quality at distant nodes.

Corresponding Author:

Farid Merahi
Department of Electrical Engineering, University Setif 1- Ferhat Abbas
Sertif, Algeria
Email: farid.merahi@univ-setif.dz

1. INTRODUCTION

Integration of renewable energy (RE) sources, such as solar and wind generators (WGs), offers numerous benefits for energy system and society as a whole [1]. Renewable energies contribute to a more sustainable electricity system by reducing dependence on fossil fuels and lowering CO_2 emissions from electricity generation, which is essential for achieving climate targets [2], [3]. In addition, the emergence of decentralized RE production units diversifies energy supply and strengthens the system's resilience to price fluctuation. Technological innovations and falling costs have made solar and wind energy competitive with conventional energy sources in many cases, giving them an increasingly important role in the international energy mix [4], [5].

The integration of wind energy affects power system stability by causing power peaks and frequency imbalances due to intermittency and the lack of natural inertia from power electronic interfaces [6], [7]. This necessitates grid modernization, including synthetic inertia and grid-forming solutions such as batteries and advanced power electronics, as well as adapted grid management for decentralized generation. Moreover, rapid wind deployment impacts short-term electricity markets, leading to reduced renewable revenues, more frequent negative prices, and increased flexibility requirements.

The complexity of the centralized electrical grid is further accentuated by the integration of decentralized RE sources as wind energy, which are being developed all over the world, as several countries

are engaged with energy transition laws for green growth [8]. For EU, the commitment has been made by all member states to increase the share of RE to reach at least 27% of the Union's energy consumption by 2030. Algeria aims to supply 30% of its energy from renewable by 2030, posing a key challenge for the centralized network to integrate these decentralized sources while maintaining balance, stability, and proper operation.

System operator will have to rethink the traditionally unidirectional network and transform it into a bidirectional one, where energy flows not only from the producer to the consumer but also from the "consumer-actor" to other consumers [9], [10]. In any case, RE do not mean the end of the existing electrical grid, which remains an important element of the increased decentralized energy model [11]. The scattering of WGs originates primarily from the fact that these energies are produced as close as possible to consumers and are therefore distributed across the territory [12]. However, this dispersion is also explained by the limited availability of large land areas, which leads to the creation of small production units. This low concentration of WG production requires electrical grid reinforcement in order to integrate these production units to consumption sites [13].

Consequently, the power system faces new challenges due to the increase in intermittent wind electricity generation which opposes to centralized generation presents a new situation that must be managed [14], [15]. The integration of WGs into the distribution network can generate various incidences, affecting the electrical variables such as the power flow, voltages at different nodes, unbalances, harmonics and stability. In addition, they can affect the network equipment by damaging the dielectrics of the cables, which can lead to voltage elevation [16], [17]. The integration of WGs into conventional power grids poses technical challenges due to the shift from mechanically synchronized generation to power-electronics-based systems [18], [19]. This transition can cause temporary or permanent overvoltages, threatening grid stability and power quality [20]. Existing studies have focused on specific effects such as flicker and harmonics [21] or circuit breaker transient parameters [22], without directly addressing overvoltage phenomena. WGs injects active and reactive power, which can increase voltage and improve profile stability. Conversely, in near substations, where voltage is generally higher, a significant injection of wind energy can cause voltage overloads, sometimes exceeding the permitted ranges.

This paper focuses on the overvoltage impact assessment due to the integration of WGs into low voltage distribution network. After describing the structure of low voltage distribution network, the expressions of voltage level at the nodes and voltage drops are formulated. Simplified models of the different elements of WGs are also presented. The studied system is simulated in MATLAB/Simulink software, under two different scenarios, without and with integration of WGs. The results, compared with the standards test feeder IEEE 33-bus system, show that integrating WGs cause voltage rise at nodes near to the connection point and improves voltage quality at distant nodes.

2. METHOD

The LV distribution network delivers electricity from a 160kVA, 20/0.4kV MV/LV transformer to end consumers at 230/400 V via overhead or underground cables, with individual connections protected by circuit breakers. The studied network has 14 nodes and 13 active and reactive power loads.

2.1. LV distribution network

A low-voltage distribution network comprises several loads located far from the source substation, as shown in Figure 1. It shows low voltage distribution configuration network shewing the different lengths and cable types (type 5 is a three-phase 4-wire cable – 3*150 mm² and a 70 mm² neutral, type 7 is a three-phase 4-wire cable - 3*95 mm² and a 50 mm² neutral). The equivalent simulation setup of the LV distribution network is also presented in Figure 1.

The simulation model is based on a complete topological representation of low-voltage network (400/230 V), where the nodes correspond to the junction points and customers, each component being characterized by its precise electrical parameters: length, type and cross-section of the conductor for calculating series impedances (R, L) according to standard formulas and shunt capacitance. Customer loads are modelled as complex powers Li (P, Q) injected at the corresponding nodes, with the possibility of a load profile over time. The simulation is implemented includes network initialization, definition of all parameters, execution of calculations and extraction of voltages.

2.2. Voltage drops

Voltage drops, which occurs, when we connect a PQ node to two bus is presented in Figure 2 and given by the (1) [23].

$$\frac{\Delta U}{U} = \frac{R.P_{+}X.Q}{U^2} \quad (1)$$

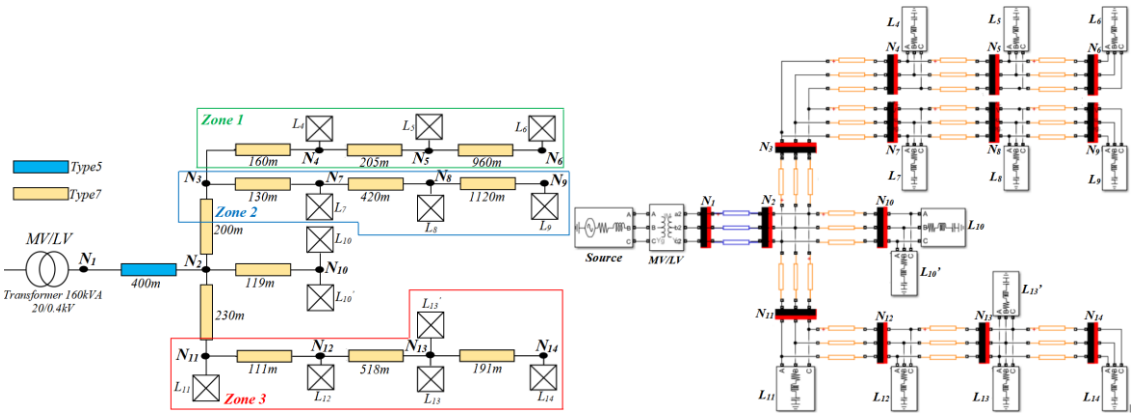

Figure 1. LV distribution network configuration and simulation setup

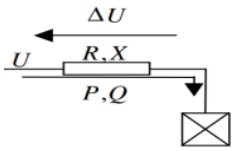

Figure 2. Voltage drops across *R*, *X* impedance

The voltage drops between the feeder and the common connection point (CCP) of the WGs through one line is expressed as (2) and (3):

$$\Delta U = R.\frac{P_N}{U_N} + X.\frac{Q_N}{U_N} \quad (2)$$

$$\Delta U = R.\frac{P_N}{U_N} + L.w.\frac{Q_N}{U_N} \quad (3)$$

where: *R*: is the total resistance of the line, *X*: is the total reactance of the line, U_N: is the voltage at the node *N*, P_N, Q_N: are the active and reactive powers at the node *N*.

The injection of energy from renewable sources into the electricity grid directly influences local voltage. Active power tends to increase voltage by reducing Joule losses on the lines, while reactive power injection has a more direct and significant impact on the voltage profile. According to the relationship $Q \propto \Delta V$, the injection of reactive power compensates for the reactive consumption of loads and lines, thereby reducing the voltage drop and leading to an increase in the voltage level at the CCP.

2.3. Network analysis

For analysis, we consider a general radial network as simple as possible shown in Figure 3, with *n* loads, *n-1* lines, a short-circuit impedance (R_1, X_1 in series with a perfect voltage source) and a distributed generator located at node N_{14}.

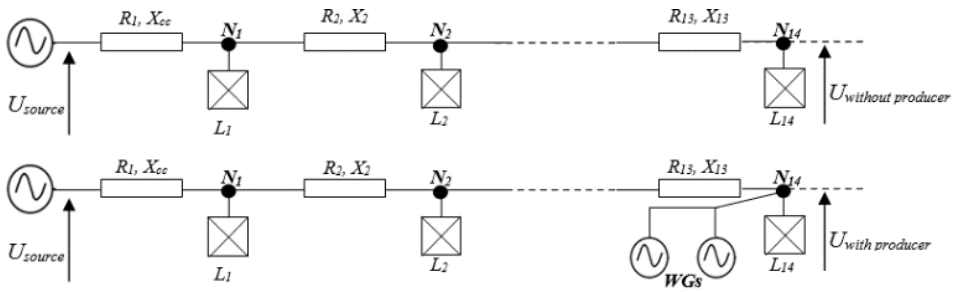

Figure 3. Network analysis with and without WGs connected to node N_{14}

In LV distribution network, a line resistance is very high than a line reactance ($R>>L$), for this reason we use this type of network where the overvoltage phenomena is easily observable. Therefore, the voltage drop will depend only on the active power as given by (4):

$$\Delta U = R.\frac{P_N}{U_N} \tag{4}$$

Thus, the voltage drop between the station source and the CCP N_j is given as [24]:

$$\Delta U(N_j) = \frac{\sum_{k=1}^{n}\left(\sum_{l=1}^{k\leq j} R_l\right).P_k + \sum_{k=1}^{n}\left(\sum_{l=1}^{k\leq j} X_l\right).Q_k}{U_{source}} \tag{5}$$

2.4. WGs configuration and model

Two WGs, each rated at 2MW and based on permanent magnet synchronous generators (PMSG), are integrated to the grid at node N_{14} via cascaded power electronic converters, as shown in Figure 4. The mathematical models of the wind turbine, PMSG, and associated power converters are described by the equations presented in [25].

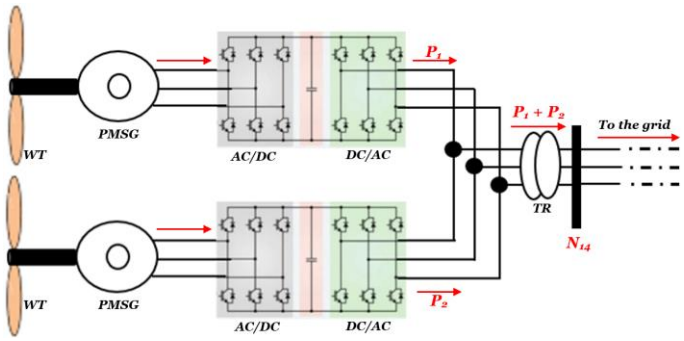

Figure 4. WGs connected LV distribution network at node N_{14}

The aerodynamic torque expression is given as (6):

$$P_t = \frac{1}{2}.C_p(\lambda,\beta).\rho.S.v^3 \tag{6}$$

Applying Park transformation and simplifications, the PMSM model becomes (7):

$$\begin{cases} v_d = R_s i_d + L_d \frac{d}{dt} i_d - \omega_r L_q i_q \\ v_q = R_s i_q + L_q \frac{d}{dt} i_q + \omega_r \left(L_d i_d + \varphi_f\right) \\ J\frac{d\Omega_r}{dt} = T_{em} - f.\Omega_r - T_r \end{cases} \tag{7}$$

Ω_r, i_d and i_q are the state variables, they can be written as (8):

$$\begin{cases} \frac{d}{dt} i_d = -\frac{R_s}{L_d} i_d + \omega_r \frac{L_q}{L_d} i_q + \frac{v_d}{L_d} \\ \frac{d}{dt} i_q = -\frac{R_s}{L_q} i_q - \omega_r \frac{L_d}{L_q} i_d - \frac{1}{L_q}\varphi_f \omega_r + \frac{v_q}{L_d} \\ \frac{d\Omega_r}{dt} = \frac{1}{J}\left(\frac{3}{2}p.\varphi_f.i_q - f.\Omega_r - T_r\right) \end{cases} \tag{8}$$

Mathematical model of the generator side converter (rectifier) is given as (9):

$$i_{red} = \frac{1}{R_s + L_s.s}.[V_a \quad V_b \quad V_c].\begin{bmatrix} S_a \\ S_b \\ S_c \end{bmatrix} \tag{9}$$

Electrical equations of the DC-bus are given by (10):

$$U_{dc} = \frac{1}{C}\int i_c \, dt \tag{10}$$

Mathematical model of grid side converter (inverter) can be written in matrix form as (11):

$$\begin{bmatrix} V_{an} \\ V_{bn} \\ V_{cn} \end{bmatrix} = \frac{U_{red}}{6} \begin{bmatrix} 2 & -1 & -1 \\ -1 & 2 & -1 \\ -1 & -1 & 2 \end{bmatrix} \begin{bmatrix} S_a \\ S_b \\ S_c \end{bmatrix} \tag{11}$$

3. RESULT AND DISCUSSION

The drop voltage calculation given by the expression (5) is applied on a three-phase low voltage network. For the study, LV network is structured into three zones: zone 1, zone 2 and zone 3. Each zone represents one distribution line. Thus, two scenarios have been simulated, the first scenario is without integration of WGs, and the second scenario is with insertion of two WGs at nodes N_{14} as shown in Figure 3.

3.1. Scenario N°1: without integration of WGs

The simulations were carried out for drop voltage calculation on each node with two load states: a state with a half load (50%) and a state with full load (100%).

- Zone 1: 50% of load

Figure 5 shows voltage profiles in different nodes of the first zone without insertion of any renewable sources. Without connection of any WG, the electrical grid is in classical operating configuration. We observe that the voltage drops along a line, mainly due to the series impedance (resistance and reactance) of the cables, causing a drop in voltage with distance and load. The lowest voltage is 0.920 pu, generally remains acceptable in many distribution standards (often > 0.9 or 0.92 pu).

We note that the decrease is not linear with distance, as the load is distributed between the nodes, not just at the end. The sharpest drop is observed between N_1 and N_2 (400 m), from 0.971 pu to 0.947 pu (a drop of 0.024 pu), then the drop slows down (between N_5 and N_6: only 0.005 pu over 960 m), suggesting that the loads between N_5 and N_6 are low or the current flowing in this section is reduced. These results serve as a reference (case without WGs) for assessing the impact of WGs on the voltage profile. With WGs, voltages are generally expected to rise at nodes close to the insertion points, thereby reducing voltage drops. Table 1 shows the numerical results of voltages at the different nodes of zone 1, according to their distance to the feeder station, with a half load (50%).

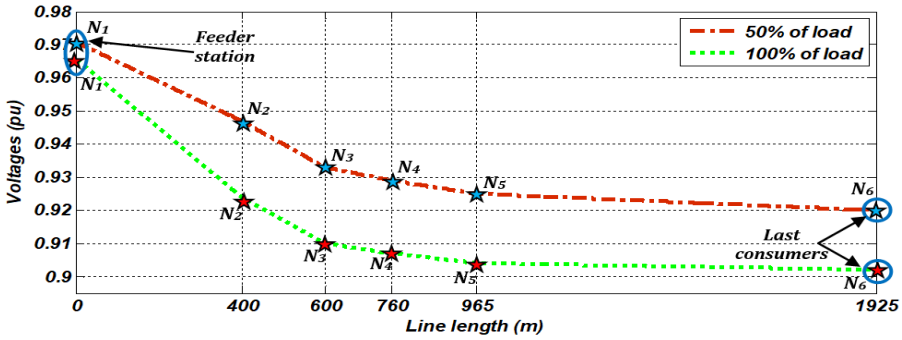

Figure 5. Voltage profiles in the first zone without WGs

Table 1. Numerical results of voltages at the nodes of the first zone with a 50% of load

Nodes	N_1	N_2	N_3	N_4	N_5	N_6
Voltages (pu)	0.971	0.947	0.933	0.929	0.925	0.920
Distance (m)	00	400	600	760	965	1925

Without decentralized production, voltage profile decreases with distance, typical of a radially loaded line. The minimum voltage (0.920 pu at N_6) is close to the lower tolerance limits (often 0.90 pu), which justifies studying ways to improve the profile, for example by inserting WGs, which inject reactive or active power and can raise the voltage.

- Zone 1: 100% of load

Table 2 shows the numerical results of voltages at the different nodes of zone 1, according to their distance to the feeder station, with a full load (100%). We observe that the voltage at node N1 is 0.966 pu it is slightly low to nominal voltage (1.000 pu), but acceptable in a loaded network. There is a gradual drop in voltage from node N1 to N6, with the voltage decreasing steadily from 0.966 pu at N1 to 0.902 pu at N6. This represents a total deviation of 0.064pu (or approximately a 6.4% drop between N1 and N6). From N3 to N6, voltages are low to 0.910 pu, reaching 0.902 pu at N6. During normal operation, a voltage lower than 0.95 pu can be considered low, or even problematic if it falls lower than 0.90 pu (according to standards). The voltages at N5 (0.904 pu) and N6 (0.902 pu) are close to the typical lower limit, the probable cause is the voltage drop is due to high distance (up to 1925 m) and high load (100%), without local compensation (no WG). Without WGs, all power must come from the upstream source (N1). This accentuates the voltage drop on distant nodes, as the current flowing through the lines is higher.

Table 2. Numerical results of voltages at the nodes of the first zone with a 100% of load

Nodes	N_1	N_2	N_3	N_4	N_5	N_6
Voltages (pu)	0.966	0.924	0.910	0.907	0.904	0.902
Distance (m)	00	400	600	760	965	1925

In this case, the network is heavily loaded and has a significant voltage drop at remote nodes. The voltages at the end of the line (N_5, N_6) are critical (≈0.90 pu), which could lead to stability or power quality problems for customers connected to these nodes. This scenario without WGs serves as a reference for evaluating the improvement brought about by the insertion of decentralized generation.

- Zone 2: 50% of load

Figure 6 shows the voltage profiles in the second zone without WGs, it shows a significant voltage drop at remote nodes. We note that all voltages are below 1.0 pu, indicating a voltage drop along the line. The further away from the source (assumed to be close to N_1), more the voltage decrease. It should be noted that the voltage drop is not strictly linear with distance, suggesting that the load is not evenly distributed; the first sections (N_1 to N_3) are probably more heavily loaded than the following ones.

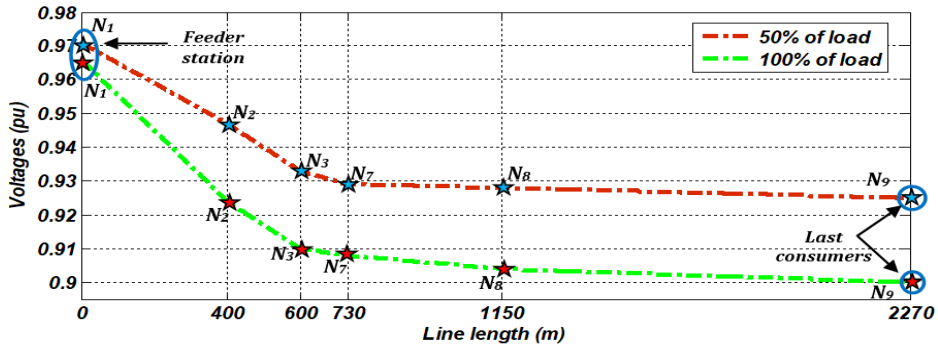

Figure 6. Voltage profiles in the second zone without WGs

Table 3 shows the numerical results of voltages at the different nodes of zone 2, according to their distance to the feeder station, with a half load (50%). Also, we note that the total voltage drops (from N1 to N9) is 4.6%. In LV distribution network, a drop >5% is often considered problematic, so, we are close to the limit. Nodes N7, N8, and N9 are critical and have voltages < 0.93 pu, this could be a problem if sensitive equipment is connected to them.

Table 3. Numerical results of voltages at the nodes of the second zone with a 50% of load

Nodes	N_1	N_2	N_3	N_7	N_8	N_9
Voltages (pu)	0.971	0.947	0.933	0.929	0.928	0.925
Distance (m)	00	400	600	730	1150	2270

In this case, the network presents a significant voltage drops, but still acceptable at 50% load. The most distant nodes are N_7, N_8, N_9 are more affected. If the load were to increase beyond 50%, measures would be necessary, such as adding WGs near to low-voltage nodes, optimizing the cross-section of conductors on the most heavily loaded sections, or using reactive energy compensation at critical locations.

- Zone 2: 100% of load

Table 4 shows the numerical results of voltages at the different nodes of zone 2, according to their distance to the feeder station, with a full load (100%).

Table 4. Numerical results of voltages at the nodes of the second zone with a 100% of load

Nodes	N_1	N_2	N_3	N_7	N_8	N_9
Voltages (pu)	0.966	0.924	0.910	0.908	0.904	0.90
Distance (m)	00	400	600	730	1150	2270

There is a gradual and significant voltage drop along the line from N_1 to N_9. N_1 (source) is at 0.966 pu, which is already slightly lower than the reference value (1.0 pu). N_9 (end) is at 0.90 pu, which is the minimum voltage recorded, it is the classic result of voltage drop in a distribution line. It can be noted that all values are low than 1.0 pu and some are very low, indicating a network under high pressure at 100% load. N1 at 0.966 pu indicates that the upstream network or the source itself may already be loaded. The maneuvering range is limited from the outset. N_9 at 0.90 pu, is critical value. According to standard EN 50160, low voltage must not fall below 0.90 pu for prolonged periods. A voltage of 0.90 pu is the acceptable lower limit and can cause electrical appliances to malfunction, poor lighting, overheating and increased losses in motors, and the risk of protection devices being triggered.

In summary, these results highlight a major failure in power quality in the network studied and provide strong technical justification for exploring the insertion of decentralized generation, such as WGs, as a means of improving network performance.

- Zone 3: 50% of load

Figure 7 shows the voltage profiles in different nodes of the third zone of two load cases (50% and 100% of load) without insertion of any renewable sources. There is a gradual and significant voltage drop along the line from N1 to N9. N1 (source) is at 0.966 pu, which is already slightly lower than the reference value (1.0 pu). N9 (end) is at 0.90 pu, which is the minimum voltage recorded, it is the classic result of voltage drop in a distribution line. A gradual voltage drop is observed along the line. The voltage at the source node (N1) is 0.971 pu (already below 1.0 pu, probably due to the upstream load or network characteristics). The lowest voltage at node N14 is 0.932 pu, representing a total drop of 0.039 pu compared to N1. So, the further away from node N1, more the voltage decreases. Table 5 shows the numerical results of voltages at the different nodes of zone 3, according to their distance to the feeder station, with a half load (50%).

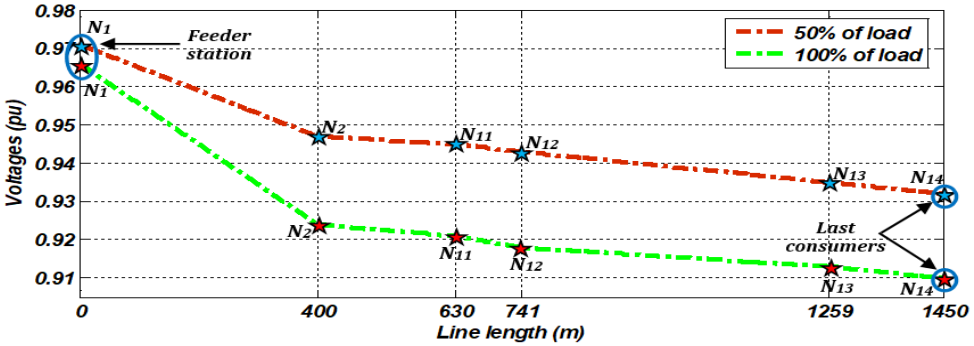

Figure 7. Voltage profiles in the third zone without WGs

Table 5. Numerical results of voltages at the nodes of the third zone with a 50% of load

Nodes	N_1	N_2	N_{11}	N_{12}	N_{13}	N_{14}
Voltages (pu)	0.971	0.947	0.945	0.943	0.935	0.932
Distance (m)	00	400	630	741	1259	1450

It is noted that the voltage drop along the lines is in line with expectations for a radial network at 50% load. It is due to the impedance of the lines (resistance and reactance) and the load currents. At 50% of load, the drops remain moderate (between 0.971 pu and 0.932 pu). In many standards (e.g., EN 50160), the voltage must generally remain between 0.90 pu and 1.10 pu in LV. In this case, 0.932 pu is still acceptable for operation at 50% of load. This case represents the basic scenario without decentralized production, where voltages are supported solely by the source node (N_1).

The network without WGs maintains acceptable voltages at 50% of load, but with a reduced margin for the most distant nodes (N_{13}, N_{14}). We note that the node N_{14} is the most critical (lowest voltage), and at full load, voltage problems could arise.

- Zone 3: 100% of load

Table 6 shows the numerical results of voltages at the different nodes of zone 3, according to their distance to the feeder station, with a full load (100%). We note that the voltage decreases with distance from N1. At the starting point (N1), the voltage is 0.966 pu, already below 1.0 pu, indicating an initial voltage drop probably due to the total connected load. At the furthest node (N14), the voltage is 0.910 pu, so, a total deviation of 0.056 pu. This gradual decrease is consistent with the effect of line resistance and reactance, as well as the load distributed along the network. In most distribution networks, the voltage must be maintained within an acceptable range (often ±5% to ±10% around 1.0 pu according to standards). Thus, 0.910 pu corresponds to -9% relative to 1.0 pu. This may be at the lower acceptable limit for some networks.

Without WGs, voltages decrease continuously along the network due to line losses and impedance. Node N_2 shows a significant drop (0.966 to 0.924 pu), indicating a heavily loaded or high-impedance section, while the lowest voltage occurs at N_{14} (0.910 pu), revealing vulnerability to additional load. The low voltage at N_1 (0.966 pu) suggests upstream network loading, which further amplifies downstream voltage drops. The minimum voltage of 0.910 pu is near standard limits, and adding wind turbines could raise voltages through active and reactive power injection, reducing line drops. Scenario 2 analyzes the improvement provided by local WG.

Table 6. Numerical results of voltages at the nodes of the third zone with a 100% of load

Nodes	N_1	N_2	N_{11}	N_{12}	N_{13}	N_{14}
Voltages (pu)	0.966	0.924	0.921	0.918	0.913	0.910
Distance (m)	00	400	630	741	1259	1450

3.2. Scenario N°2: with integration of WGs

Scenario N°2 consists to integrate two WGs at the node N_{14} according to the recommendation mentioned at the end of the first scenario, and assess the improvement brought about by local production. This part, includes a comparison with IEEE 33-Bus system for each case.

- Zone 1: 50% of load

Figure 8 shows voltage profiles in different nodes of the first zone for two load cases (50% and 100%) with insertion of two WGs at node N_{14}. Table 7 shows the numerical results of voltages at the different nodes of the first zone, according to their distance to the feeder station, with a half load (50%).

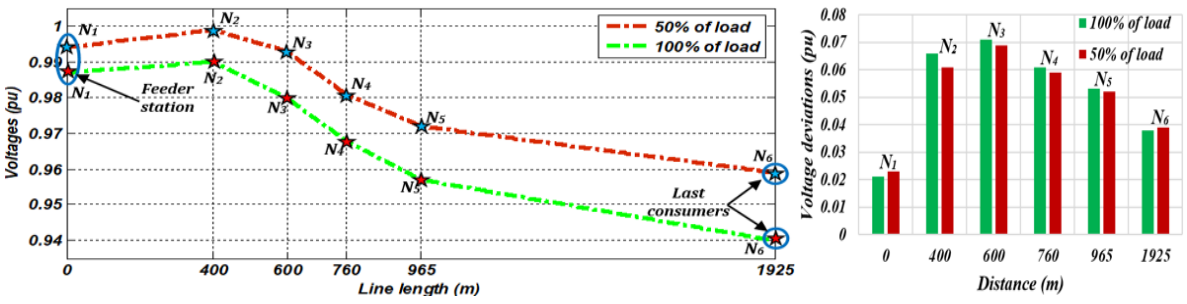

Figure 8. Voltage profiles in the 1st zone in presence of WGs connected at N_{14}, and voltage deviations

Table 7. Numerical results of voltages at the nodes of the first zone with a 50% of load

Nodes	N_1	N_2	N_3	N_4	N_5	N_6
Voltages (pu)	0.994	1.008	1.002	0.988	0.977	0.959
Distance (m)	00	400	600	760	965	1925
Voltage deviations (pu)	**0.023**	**0.061**	**0.069**	**0.059**	**0.052**	**0.039**

We note that at the source node (N_1) the voltage is 0.994 pu, which is slightly below 1.0 pu. There is a maximum voltage drop of approximately 3.5% between N_2 (1.008 pu) and N_6 (0.959 pu). N_2 has the highest voltage (1.008 pu) despite N_1 = 0.994 pu, which probably indicates power injection from the WGs. The voltage at N_3 (1.002 pu) and N_4 (0.988 pu) show a transition, and the most distant nodes (N_5 = 0.977 pu, N_6 = 0.959 pu) have the lowest voltages.

WGs have a positive impact on the voltage profile, with N_2 higher than N_1 due to active and reactive power injection. Even at 1925m, the voltage remains at 0.959 pu, within acceptable limits. Overall, WGs reduce voltage drops, especially near their connection points, and voltages generally stay within standard limits (0.95–1.05 pu), indicating the system is well-sized for this load.

The comparison with IEEE 33-bus is limited by the difference in scale and topology, but the principles observed (improvement in voltages through WGs) are consistent with the literature on distribution networks with distributed generation.

- Zone 1: 100% of load

Table 8 shows the numerical results of voltages at the different nodes of the first zone, according to their distance to the feeder station, with a full load (100%). There is a 0.047 pu voltage drop from node N1 to the furthest node N6, keeping voltages within acceptable limits (0.95–1.05 pu), though N6 (0.940 pu) is near the lower limit. WGs provide voltage support via reactive power, allowing N1 to operate below 1.0 pu while maintaining a viable profile to N6. N6 is the weakest point and requires careful monitoring, as load increases or wind variability could push its voltage below standard limits.

Compared to the standard IEEE 33-bus network, the worst-case voltage is generally found at node 18 (the furthest away), with a voltage of approximately 0.903 to 0.913 pu. The profile along the main section shows a continuous voltage drop, similar to the trend observed in our case, but more pronounced due to the total length of the network.

Table 8. Numerical results of voltages at the nodes of the first zone with a 100% of load

Nodes	N_1	N_2	N_3	N_4	N_5	N_6
Voltages (pu)	0.987	0.99	0.981	0.968	0.957	0.94
Distance(m)	00	400	600	760	965	1925
Voltage deviations (pu)	**0.021**	**0.066**	**0.071**	**0.061**	**0.053**	**0.038**

- Zone 2: 50% of load

Figure 9 shows voltage profiles in different nodes of the second zone for two load cases (50% and 100%) in presence of two WGs connected at node N_{14}. Table 9 shows the numerical results of voltages at the different nodes of the second zone, according to their distance to the feeder station, with a full load (50%).

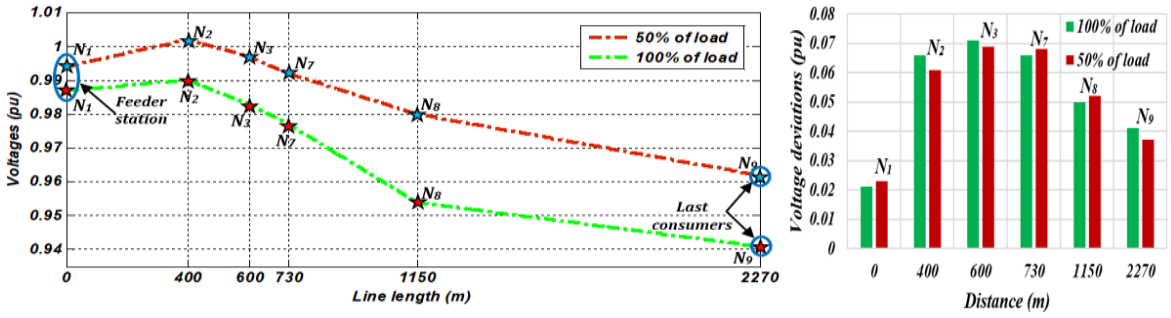

Figure 9. Voltage profiles in the 2nd zone in presence of WGs connected at node N_{14}, and voltage deviations

Table 9. Numerical results of voltages at the nodes of the second zone with a 50% of load

Nodes	N_1	N_2	N_3	N_7	N_8	N_9
Voltages (pu)	0.994	1.008	1.002	0.997	0.98	0.962
Distance (m)	00	400	600	730	1150	2270
Voltage deviations (pu)	0.023	0.061	0.069	0.068	0.052	0.037

Wind power injected at node N_{14} raises voltages at upstream nodes, with N_2 (1.008 pu) and N_3 (1.002 pu) slightly above 1.0 pu, indicating localized overvoltage, while N_1 rises to 0.994 pu. Although WGs

improve the overall voltage profile, voltage drops at distant nodes are not fully compensated. The reactive and active power from the turbines provides the strongest support to nearby nodes, with the effect diminishing with electrical distance. Compared to the 33-bus IEEE baseline case, this system has a significantly healthier and flatter voltage profile. This is due to a combination of two factors, a load that is reduced by half, naturally decreasing voltage drops, and energy injection from the wind turbines at node N_{14}, which actively compensates for losses and supports the voltage, even creating slight local voltage rises. It should be noted that the minimum voltage of 0.962 pu, although acceptable, indicates that problems could arise at 100% load or if the WGs are not producing power.

- Zone 2: 100% of load

Table 10. Shows the numerical results of voltages at the different nodes of the second zone, according to their distance to the feeder station, with a full load (100%). Voltage generally decreases with distance from the source, except between N1 and N3 (0.987–0.998 pu). After N3, it drops sharply to 0.941 pu at N9. Wind injection at N14 supports voltages nearby, keeping N1–N3 close to 1.0 pu, but has limited effect on distant nodes like N8 and N9.

Table 10. Numerical results of voltages at the nodes of the second zone with a 100% of load

Nodes	N_1	N_2	N_3	N_7	N_8	N_9
Voltages (pu)	0.987	0.99	0.981	0.973	0.954	0.941
Distance (m)	00	400	600	730	1150	2270
Voltage deviations (pu)	0.021	0.066	0.071	0.066	0.05	0.041

In the IEEE 33-bus network, minimum voltages without distributed generation are around 0.903–0.913 pu at node 18. With wind power injected at node N_{14}, the minimum voltage rises to 0.941 pu at node N_9, improving the overall voltage profile. Voltages at all nodes increase compared to the base case, and the minimum remains within acceptable standards.

- Zone 3: 50% of load

Figure 10 shows the voltage profiles in different nodes of the third zone (zone 3) for two load cases (50% and 100%) in presence of two WGs connected at node N_{14}.

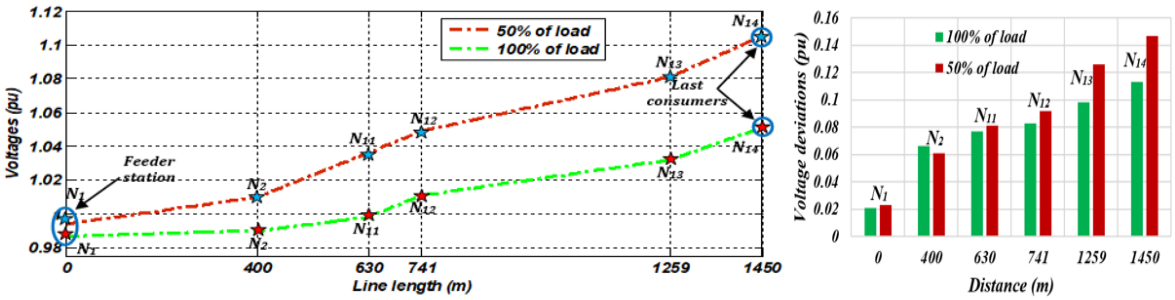

Figure 10. Voltage profiles in the 3rd zone in presence of WGs connected at N_{14}, and voltage deviations

Contrary to a typical case without WGs, where the voltage drops gradually along a line, we observe a continuous and significant increase in voltage from N_1 (0.994 pu) to N_{14} (1.079 pu). This increase is directly attributable to the injection of active power by the WGs at node N_{14}. This injection reduces the power flow from the main source (at node N_1), or even reverses it, creating a power flow towards the source. This induces a voltage drop of opposite sign along the line, which results in a voltage rise.

The voltage at node N_{14} reaches 1.079 pu (+7.9% above nominal), potentially exceeding standard limits (e.g., EN 50160), highlighting the challenge of voltage rise at line ends during high wind production and low load. This fundamental change in grid dynamics moves the system from a traditional one-way power flow to a more complex active network. Voltages exceeding equipment insulation limits can lead to premature aging and failure of transformers, cables, and other assets.

Table 11 shows the numerical results of voltages at the different nodes of the third zone, according to their distance to the feeder station, with a full load (50%).

Table 11. Numerical results of voltages at the nodes of the third zone with a 50% of load

Nodes	N_1	N_2	N_{11}	N_{12}	N_{13}	N_{14}
Voltages (pu)	0.994	1.008	1.028	1.035	1.061	1.079
Distance (m)	00	400	630	741	1259	1450
Voltage deviations (pu)	0.023	0.061	0.081	0.092	0.126	0.147

Table 11 highlights a shift in the IEEE 33-bus network: with WGs integrated, especially at line ends during low load, the classic challenge of boosting end-of-line voltage is replaced by the modern issue of controlling voltage profile.

- Zone 3: 100% of load

Table 12 shows the numerical results of voltages at the different nodes of the third zone, according to their distance to the feeder station, with a full load (100%). The integration of WGs at node N14 injects active and reactive power, locally raising the voltage to 1.023 pu, while the lowest voltage at N1 (0.987 pu) remains acceptable. Voltage variations along the line reflect power flow toward N1, with line losses reducing voltages farther from the injection point. The voltage profile is influenced more by load distribution and network topology than by distance alone.

Table 12. Numerical results of voltages at the nodes of the third zone with a 100% of load

Nodes	N_1	N_2	N_{11}	N_{12}	N_{13}	N_{14}
Voltages (pu)	0.987	0.99	0.998	1.001	1.011	1.023
Distance (m)	00	400	630	741	1259	1450
Voltage deviations (pu)	0.021	0.066	0.077	0.083	0.098	0.113

In IEEE 33-bus system with radial distribution, voltage generally decreases from the source substation to the ends. In this study, wind power injection reverses this trend near node N_{14}. The 33-bus IEEE often has voltages between 0.90 pu and 1.00 pu at nominal load without distributed generation. For the studied case, the results (0.987 to 1.023 pu) show an improvement due to wind power injection. In both cases, the insertion of WGs cause a local voltage rise, requiring control to avoid exceeding limits (1.05 pu). In this case, the results show all voltages close to or above 1.0 pu, indicating effective voltage support by the WGs. In the 33-bus IEEE system without distributed generation, end-of-line voltages are often below 0.95 pu.

We deduce that the insertion of WGs at node N_{14} has a beneficial effect on the voltage profile in the studied area, keeping all voltages within a healthy range. The comparison with the IEEE 33-bus model shows how distributed generation can reverse traditional voltage profiles, reducing losses and improving stability, but requiring careful management to avoid local overvoltages. Sensitivity analysis identifies the most unfavorable scenarios and assesses the robustness of the grid, providing valuable information for the design of compensation measures, congestion management and the secure integration of renewable energies.

Tables 13-16 present the parameters used in the simulation, including the HV/LV transformer parameters, electrical grid line parameters, low-voltage network load parameters, and wind turbine generator parameters.

Table 13. Transformer HV/LV parameters

Parameters		Values
Nominal power (S)		160 kVA
Magnetisation resistance (R_m)		3750 Ω
Magnetisation inductance (L_m)		11937 H
Primary winding	Primary voltage (V_1)	20 kV
	Resistance (R_1)	110.25 Ω
	Inductance (L_1)	0.889 H
Secondary winding	Secondary voltage (V_2)	0.4 kV
	Resistance (R_2)	0.001 Ω
	Inductance (L_2)	0.003 mH

Table 14. Electrical grid line parameters

Parameters	Values	Parameters	Values
r_1 (Ohms/km)	0.01273	r_0 (Ohms/km)	0.3864
l_1 (mH/km)	0.9337	l_0 (mH/km)	4.1264
c_1 (µF/km)	0.01274	c_0 (µF/km)	0.007751

Table 15. Low-voltage network load parameters

	Load										
Nodes	P(kW)	Q(kVar)	Nodes	P(kW)	Q(kVar)	Nodes	P(kW)	Q(kVar)	Nodes	P(kW)	Q(kVar)
N_3	47	17.5	N_6	4.9	1.8	N_9	1.1	0.2	N_{12}	4.2	1.6
N_4	6.3	2.3	N_7	1.3	0.5	N_{10}	7	2.6	N_{13}	7.2	2.7
N_5	2.2	0.8	N_8	1.2	0.4	N_{11}	7.3	2.7	N_{14}	6.3	2.3

Table 16. Parameters of wind turbine energy generators

Parameters	Values	Parameters	Values	Parameters	Values
Apparent power (S)	120VA	Statoric reactance (X_a)	0.0101pu	Homopolar reactance (x_h)	1
Nominal voltage (Vn)	208V	Resistance of D-axis damper (r_D)	0.012pu	Leak resistance (r_L)	0.1983pu
Maximal current (I_m)	0.33A	Reactance of D-axis damper (x_D)	0.669pu	Leak reactance (x''_d)	0.0295pu
Frequency (f)	50Hz	Resistance of Q-axis damper (r_Q)	0.0073pu	Mutual reactance at axis d (X_d)	0.350pu
Rotation speed (N)	120rpm	Reactance of Q-axis damper (x_Q)	0.1352pu	Mutual reactance at axis q (X_q)	0.3417pu
Statoric resistance (r_a)	0.0198pu	Homopolar resistance (r_h)	1	Kany reactance (X_{kf1})	-0.0081pu

4. CONCLUSION

This work focuses on assessing the overvoltage impact caused by the integration of WGs into electricity grids. This assessment shows that overvoltage mainly manifests themselves in the form of temporary and sustained increases in voltage, particularly during periods of high wind and low consumption, which put the grid in a critical state. Two scenarios have been presented, simulated and discussed; they can serve as proof of concept for a section of a more complex network. The first scenario without WGs serves as a good reference for evaluating the improvement brought about by the integration of decentralized generation. Second scenario with integration of WGs has been detailed, improves voltage profile in some nodes, but requiring careful management to avoid local voltage rises, which can lead to premature aging and failure of transformers, cables, and other assets**.** Compared to IEEE 33-node without DG, the studied case shows significantly better voltages, so the WGs plays a positive role, but this is not sufficient to completely eliminate the voltage drop at the end of the line.

The comparison with IEEE 33-bus system highlights the profound impact of decentralized RE on the dynamics of electricity grids, which requires new control, reactive power compensation, protection and planning strategies. Controlling the impact of electrical surges is therefore a technical and economic challenge for the large-scale deployment of wind energy, requiring appropriate protection and a detailed study of electrical compatibility with the grid.

ACKNOWLEDGMENTS

I would like to express my gratitude and appreciation for LAS members. whose guidance, support and encouragement has been invaluable throughout this study. I would also like to thank PRFU researchers' team whose have been a great source of support.

FUNDING INFORMATION

Authors state no funding involved.

AUTHOR CONTRIBUTIONS STATEMENT

This journal uses the Contributor Roles Taxonomy (CRediT) to recognize individual author contributions, reduce authorship disputes, and facilitate collaboration.

Name of Author	C	M	So	Va	Fo	I	R	D	O	E	Vi	Su	P	Fu
Farid Merahi	✓	✓	✓		✓	✓	✓	✓	✓	✓	✓			✓
Abd Essalam Badoud		✓		✓		✓		✓	✓		✓	✓	✓	

C : **C**onceptualization
M : **M**ethodology
So : **So**ftware
Va : **Va**lidation
Fo : **Fo**rmal analysis
I : **I**nvestigation
R : **R**esources
D : **D**ata Curation
O : Writing - **O**riginal Draft
E : Writing - Review & **E**diting
Vi : **Vi**sualization
Su : **Su**pervision
P : **P**roject administration
Fu : **Fu**nding acquisition

CONFLICT OF INTEREST STATEMENT

Authors state no conflict of interest.

INFORMED CONSENT

We have obtained informed consent from all individuals included in this study.

ETHICAL APPROVAL

Authors state no people or animal data are used.

DATA AVAILABILITY

Data availability is not applicable to this paper as no new data were created in this study.

REFERENCES

[1] A. Hirsch, Y. Parag, and J. Guerrero, "Microgrids: A review of technologies, key drivers, and outstanding issues," *Renewable and Sustainable Energy Reviews*, vol. 90, pp. 402–411, Jul. 2018, doi: 10.1016/j.rser.2018.03.040.

[2] A. O. Abbas and B. H. Chowdhury, "Using customer-side resources for market-based transmission and distribution level grid services – A review," *International Journal of Electrical Power and Energy System*s, vol. 125, p. 106480, Feb. 2021, doi: 10.1016/j.ijepes.2020.106480.

[3] E. Mengelkamp, J. Gärttner, K. Rock, S. Kessler, L. Orsini, and C. Weinhardt, "Designing microgrid energy markets," *Applied Energy*, vol. 210, pp. 870–880, Jan. 2018, doi: 10.1016/j.apenergy.2017.06.054.

[4] D. P. Mishra, B. S. Panda, N. S. Mallik, S. Kar, N. C. Giri, and S. R. Salkuti, "Demand side management in a microgrid to reduce the peak consumption cost," *International Journal of Power Electronics and Drive Systems (IJPEDS)*, vol. 14, no. 2, pp. 819–826, Jun. 2023, doi: 10.11591/ijpeds.v14.i2.pp819-826.

[5] H. J. Queen, J. J., and D. T. J., "Comparative techno-economic analysis of power system with and without renewable energy sources," *Indonesian Journal of Electrical Engineering and Computer Science (IJEECS)*, vol. 24, no. 3, pp. 1260–1268, Dec. 2021, doi: 10.11591/ijeecs.v24.i3.pp1260-1268.

[6] S. Bahramara, A. Mazza, G. Chicco, M. Shafie-khah, and J. P. S. Catalão, "Comprehensive review on the decision-making frameworks referring to the distribution network operation problem in the presence of distributed energy resources and microgrids," *International Journal of Electrical Power and Energy Systems*, vol. 115, p. 105466, Feb. 2020, doi: 10.1016/j.ijepes.2019.105466.

[7] I. Alotaibi, M. A. Abido, M. Khalid, and A. V. Savkin, "A comprehensive review of recent advances in smart grids: A sustainable future with renewable energy resources," *Energies*, vol. 13, no. 23, p. 6269, Nov. 2020, doi: 10.3390/en13236269.

[8] S. Choudhury, "A comprehensive review on issues, investigations, control and protection trends, technical challenges and future directions for microgrid technology," *International Transactions on Electrical Energy Systems*, vol. 30, no. 9, Sep. 2020, doi: 10.1002/2050-7038.12446.

[9] Z. Yu, Z. Wang, and J. Kou, "A novel decentralized control strategy for microgrids, combining renewable energy resources," in *Proceedings of the 2024 IEEE 2nd International Conference on Electrical, Automation and Computer Engineering (ICEACE)*, Changchun, China, Dec. 2024, pp. 1366–1373, doi: 10.1109/ICEACE63551.2024.10898376.

[10] F. Azeem, G. B. Narejo, and U. A. Shah, "Integration of renewable distributed generation with storage and demand side load management in rural islanded microgrid," *Energy Efficiency*, vol. 13, no. 2, pp. 217–235, Feb. 2020, doi: 10.1007/s12053-018-9747-0.

[11] D. I. Brandao, T. Caldognetto, F. P. Marafao, M. G. Simoes, J. A. Pomilio, and P. Tenti, "Centralized control of distributed single-phase inverters arbitrarily connected to three-phase four-wire microgrids," *IEEE Transactions on Smart Grid*, vol. 8, no. 1, pp. 437–446, Jan. 2017, doi: 10.1109/TSG.2016.2586744.

[12] S. Tuo, D. Jiandong, and X. Ma, "Active and reactive power coordination control strategy of overvoltage for distributed PV integrated grid," *The Journal of Engineering*, vol. 2019, no. 16, pp. 2960–2964, Mar. 2019, doi: 10.1049/joe.2018.8913.

[13] D. Gielen, F. Boshell, D. Saygin, M. D. Bazilian, N. Wagner, and R. Gorini, "The role of renewable energy in the global energy transformation," *Energy Strategy Reviews*, vol. 24, pp. 38–50, Apr. 2019, doi: 10.1016/j.esr.2019.01.006.

[14] Z. Pató and T. Mandel, "Energy efficiency first in the power sector: Incentivising consumers and network companies," *Energy Efficiency*, vol. 15, no. 8, p. 57, Dec. 2022, doi: 10.1007/s12053-022-10062-9.

[15] S. Dash, S. Chakravarty, N. C. Giri, and R. Khargotra, "Evaluating sustainable wind energy sources with multiple criteria decision-making (MCDM) techniques," *Computers and Electrical Engineering*, vol. 123, p. 110285, Apr. 2025, doi: 10.1016/j.compeleceng.2025.110285.

[16] T. J. Hammons, "Integrating renewable energy sources into European grids," *International Journal of Electrical Power and Energy Systems*, vol. 30, no. 8, pp. 462–475, Oct. 2008, doi: 10.1016/j.ijepes.2008.04.010.

[17] J. P. Holguin, D. C. Rodriguez, and G. Ramos, "Reverse power flow (RPF) detection and impact on protection coordination of distribution systems," *IEEE Transactions on Industry Applications*, vol. 56, no. 3, pp. 2393–2401, May 2020, doi: 10.1109/TIA.2020.2969640.

[18] J. Caballero-Peña, C. Cadena-Zarate, A. Parrado-Duque, and G. Osma-Pinto, "Distributed energy resources on distribution networks: A systematic review of modelling, simulation, metrics, and impacts," *International Journal of Electrical Power and Energy Systems*, vol. 138, p. 107900, Jun. 2022, doi: 10.1016/j.ijepes.2021.107900.

[19] E. J. Coster, J. M. A. Myrzik, B. Kruimer, and W. L. Kling, "Integration issues of distributed generation in distribution grids," *Proceedings of the IEEE*, vol. 99, no. 1, pp. 28–39, Jan. 2011, doi: 10.1109/JPROC.2010.2052776.

[20] S. Adel and C. Rachid, "Enhancement of a voltage drop in a low-voltage grid by the contribution of a hybrid PV-wind turbine generator," *Journal of The Institution of Engineers (India): Series B*, vol. 102, no. 5, pp. 947–956, Oct. 2021, doi: 10.1007/s40031-021-00614-5.

[21] O. Benzohra, S. S. Echcharqaouy, F. Fraija, and D. Saifaoui, "Integrating wind energy into the power grid: Impact and solutions," *Materials Today: Proceedings*, vol. 30, pp. 987–992, 2020, doi: 10.1016/j.matpr.2020.04.363.
[22] M. Heydari and A. A. Razi-Kazemi, "Impacts of various wind turbine generators on transient recovery voltage in a medium voltage power network," in *Proceedings of the 2022 30th International Conference on Electrical Engineering (ICEE)*, Tehran, Iran, May 2022, pp. 102–107, doi: 10.1109/ICEE55646.2022.9827052.
[23] M. Emmanuel and R. Rayudu, "The impact of single-phase grid-connected distributed photovoltaic systems on the distribution network using P–Q and P–V models," *International Journal of Electrical Power and Energy Systems*, vol. 91, pp. 20–33, Oct. 2017, doi: 10.1016/j.ijepes.2017.03.001.
[24] A. Bouakra, F. Slaoui-Hasnaoui, M. Rustom, and S. Georges, "Voltage regulation of electric power network interconnected with wind energy distributed generations," in *Proceedings of the 2017 IEEE Second International Conference on DC Microgrids (ICDCM*), Nuremberg, Germany, Jun. 2017, pp. 387–392, doi: 10.1109/ICDCM.2017.8001075.
[25] C. Qu, Z. Lin, J. Liu, Y. Yu, X. Tian, and Z. Yuan, "Modeling and hardware-in-the-loop implementation of real-time aero-elastic-electrical co-simulation platform for PMSG wind turbine," *Applied Energy*, vol. 359, p. 122777, Apr. 2024, doi: 10.1016/j.apenergy.2024.122777.

BIOGRAPHIES OF AUTHORS

Farid Merahi associate professor at the department of Electrical Engineering, University Setif 1, Ferhat Abbas, Setif, Algeria. He Holds a Ph.D. degree in Control Engineering with specialization electrical control systems from the National Polytechnic High School of Algiers in collaboration with PEARL Laboratory of Malaya University, Malaysia in 2014. He is used to hold several administrative posts at the Department of Electrical Engineering, University Setif 1, such as the head of the speciality: Electrical control from 2015 to 2018, including the Head of Department of Electrical Engineering from 2022 until now, and member of LAS Laboratory from 2012 to 2025. His research areas are control systems, renewable energies, integration of renewable sources into the power system. His research interests include electrical machine control, power electronic converters and energy sustainability. He can be contacted at email: farid.merahi@univ-setif.dz.

Abd Essalam Badoud Prof. Dr. Ing. BADOUD Abd Essalam was born in Setif, he earned his engineering degree in Automatic Control from University of Setif 1 - Ferhat Abbas in 2006, followed by a Magister degree in 2009 and a Ph.D. in 2014 from the same institution. Currently, he serves as a full professor in the Department of automatic and intelligent systems at university of Setif 1 - Ferhat Abbas and is an active member of the Automatic Laboratory of Setif (LAS). His research focuses on power converter control, maximum power point tracking (MPPT), renewable energy, and energy efficiency. He has authored and co-authored over 150 publications in academic journals and proceedings, along with three books, and supervising over 10 Ph.D. students who have graduated under his guidance. He is an editorial board member for many journals. He can be contacted at email: badoudabde@univ-setif.dz.